

ERS-ENVISAT Permanent Scatterers

Daniele Perissin, Claudio Prati, Fabio Rocca
Dipartimento di Elettronica e Informazione
Politecnico di Milano
Milano, Italy
perissin@elet.polimi.it

Alessandro Ferretti
Tele-Rilevamento Europa – T.R.E.
www.treuropa.com
Milano, Italy
alessandro.ferretti@treuropa.com

Abstract— The phase time series of a perfect point-wise Permanent Scatterer (PS) would show a phase jump passing from ERS to ENVISAT SAR images. A PS analysis has been carried out on a dataset including both ERS and ENVISAT images. For each PS, elevation, LOS velocity and phase jump have been jointly estimated and removed, allowing the identification of the atmospheric phase screen. The PS population so found represents the intersection of ERS and ENVISAT PS populations. The probability of natural targets to behave as PS both in ERS and ENVISAT has been analyzed as a function of their Radar Cross-Section, acquisition geometry and amplitude. Distributed targets with a narrow backscattering lobe pointed towards the first sensor (ERS) are not coherently observed by the second one (ENVISAT), whereas point-wise targets (e.g. natural corner reflectors, dihedrals and small mirrors) will remain coherent in both cases. Experimental results have been carried out on a data set of 69 ERS images and 7 ENVISAT images (ERS-like mode) on Milano over a 20 km side area.

Keywords— Permanent Scatterers, Differential SAR Interferometry, ENVISAT.

I. INTRODUCTION

The Permanent Scatterers (PS) technique has been recognized to be a powerful and fully operational satellite SAR remote sensing tool. The peculiarity of this approach is the possibility to exploit interferometric SAR images with very long baseline over a several years time interval independently of atmospheric disturbances [1], [2], [3]. As ENVISAT was launched in March 2002, updating results obtained by means of a PS analysis on ERS interferometric data with ENVISAT ASAR images became a major issue. The feasibility of such a goal was studied in [4] and preliminary results over a small area were reported in [5]. In this paper the theoretical bases are recalled and the results on the processed area of Milan (~400 sqkm) are shown and discussed.

II. POINT-WISE THEORY

The main difference between ERS-1/2 and ENVISAT ERS-like acquisitions is in the carrier frequency (5.3 GHz for ERS-1/2 and 5.331 GHz for ENVISAT). In the case of point scatterers, the 30MHz frequency gap generates a new phase term on interferograms that changes from point to point but remains constant in all the acquisitions.

For a given PS with slant range position and elevation respectively Δr and Δq (both relative to the center of the

sampling cell taken as origin of the coordinates), the ERS/ENVISAT interferometric phase can be expressed as:

$$\Delta\phi = \frac{4\pi}{c} \left\{ \Delta r \Delta f + \Delta r \frac{f_0 B_n}{r_M \tan \theta} + \Delta q \frac{f_0 B_n}{r_M \sin \theta} \right\} \quad (1)$$

where c is the light speed, B_n the normal baseline, r_M the sensor-target distance, θ the incidence angle, f_0 the ERS carrier frequency and Δf the frequency gap between ENVISAT and ERS. In (1) the new term $\Delta f \Delta r$ appears besides the usual flat Earth and topographic phase terms. Given the 30 MHz frequency shift, this new term introduces a linear phase variation of about 4π across the slant range resolution cell. Therefore, the location of the scatterer within the cell has to be known with about 1m accuracy, to be able to predict its interferometric phase within one radians accuracy. This phase term is called Location Phase Screen (LPS).

III. EXPERIMENTAL RESULTS

The chosen dataset includes 69 ERS and 7 ENVISAT images. The processed area covers a 20 km side square around the centre of Milan. An ERS common master image is selected to minimize the dispersion of the normal baseline values of all the interferograms. All the acquisitions are registered on the common master grid taking into account the differences in the PRFs and in the sampling frequencies. PS candidates (PSC) are selected setting a threshold on the amplitude stability index [1]. For each PSC the phase terms connected to the relative elevation, to the linear motion and to the frequency gap are then jointly estimated and removed. Phase residuals depend only on the atmosphere and noise. Finally, the Atmospheric Phase Screen (APS) is estimated from the residual phases exploiting its spatial correlation. Once the APS of each interferogram is estimated and compensated, PS are detected on a pixel by pixel basis. The coherence of each PS is then computed on the ERS and ENVISAT datasets separately in order to estimate their survival rate when the radar central frequency changes. In figures 1 and 2 two examples of time series are shown. The jump of phase connected to the LPS has been estimated but not removed for visualization purposes.

In Table I the main results of the coherence analysis and PS survival rate are reported. The number of PS having ERS coherence (estimated on 69 ERS images) greater than the value indicated in the first column is reported in the second column. The third column reports the number of PS showing a

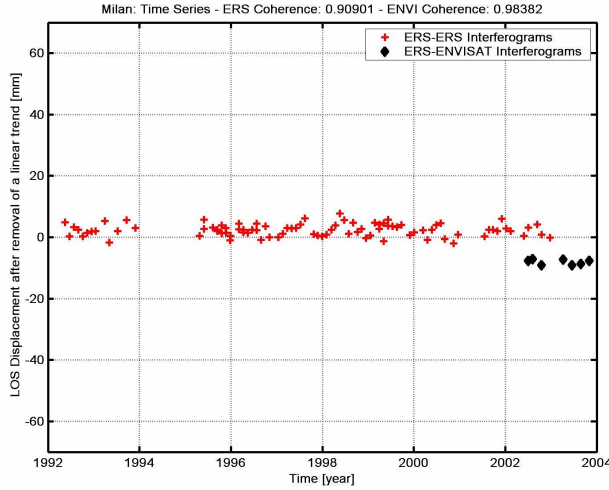


Figure 1. PS time series. ERS-ERS interferograms (red points) and ERS-ENVISAT interferograms (black points).

coherence greater than that indicated in the first column on both ERS (69 images) and ENVISAT (7 images) time series. The PS survival rate is shown in the last column of Table I. A more detailed analysis of the PS survival rate is shown in figure 3. Here the ERS coherence histogram of PSs showing coherence greater than 0.8 is compared with the ENVISAT coherence histogram of the same PSs.

TABLE I. SURVIVAL RATE FOR DIFFERENT COHERENCES

COHERENCE	ERS (NI=69)	ENVISAT (NI=7)	SURVIVAL RATE
0.80	82300	52617	64%
0.85	60888	32935	54%
0.90	26124	12215	48%
0.95	2820	833	30%

IV. RESULTS ANALYSIS

The results reported in the previous section state that more than 60% of PS is still coherent in ENVISAT acquisitions. We are interested now in understanding which objects behave as permanent scatterers in both sensors and which are the reasons of the limited survival rate. A possible explanation is that the PS are not perfectly pointwise and that their spatial extension

introduces decorrelation passing from ERS to ENVISAT surveys. We thus focused our analysis to those ERS PSs (about 10% of the total [5]) that show a *sinc* type amplitude behavior as a function of the baseline (looking angle). This amplitude behavior represents the backscattering radiation pattern of the PS at the ERS frequency. The width of the cardinal sine is therefore inversely proportional to the spatial extension of the PS, whereas the portion of radiation pattern illuminated by the radar gives information on its orientation.

The spectral shift principle [6] can be exploited to predict the radiation pattern of such partially distributed PSs when passing from ERS to ENVISAT central frequency. The spectral shift principle states an equivalence between a variation in looking angle and central frequency. This equivalence leads to the expression of the normal baseline that compensates for the ERS/ENVISAT frequency gap $\Delta f = -31\text{MHz}$

$$B_n = \frac{\Delta f}{f_0} r_M \tan(\theta - \alpha) \quad (2)$$

In (2) θ is the off-nadir angle and α the local ground slope. The compensation baseline for flat terrain is about -2km . This

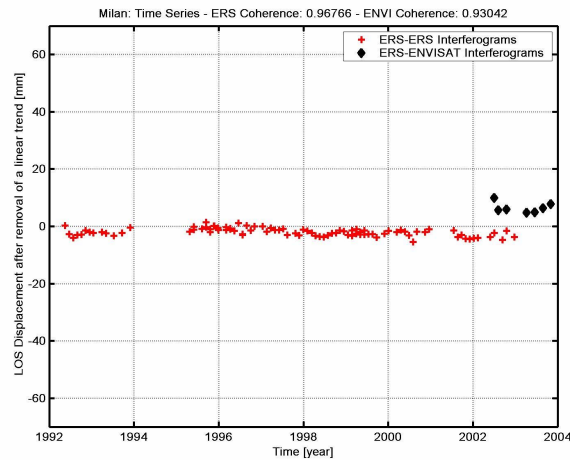


Figure 2. PS time series. ERS-ERS interferograms (red points) and ERS-ENVISAT interferograms (black points).

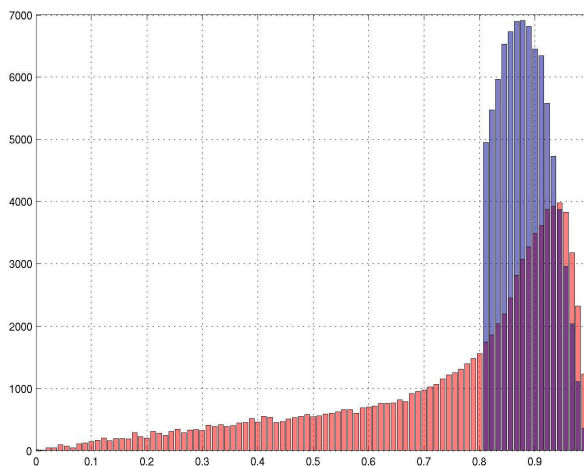


Figure 3. ERS (blue) and ENVISAT (red) PS coherence histograms.

means that at the compensation baseline ENVISAT observes an object as it would have been observed by ERS at zero baseline.

In figures 4 and 5 two examples of the PS amplitudes as a function of the baseline are shown. Following the spectral shift principle ENVISAT data are shifted by the compensation baseline. From the examples in figures 4 and 5 it is shown that the ERS PS radiation pattern is consistently continued by the ENVISAT measurements. This happens for almost all the ERS PSs that show a *sinc* type radiation pattern. However only 60~70% of such PSs survive passing from ERS to ENVISAT (almost the same survival rate of the whole PS set). A possible explanation of such a behavior (to be checked when more ENVISAT surveys will be available) is that in some case the radiation pattern illuminated by ENVISAT is close to a zero of the *sinc* (as in figure 4) and the ENVISAT PS phase dispersion is high. In other cases the radiation pattern illuminated by ENVISAT is around a local maximum (as in figure 5) and the ENVISAT PS phase dispersion is low.

As far as an explanation of the survival rate of the

remaining 90% of the ERS PSs is concerned, we have not a clear answer at the moment. Further surveys will help to get through the problem, in particular when a good statistic of ENVISAT acquisitions will be available.

Finally, it has been observed that the PS surviving probability increases with the PS Radar Cross-Section (RCS) as shown in figure 6. This is reasonable since for larger PS RCS a smaller clutter influence is expected also on the side lobes of the PS radiation pattern.

V. CONCLUSIONS

It has been demonstrated that ESA-ERS C-band archive can be continued in new ENVISAT acquisitions. ENVISAT-ASAR can be usefully exploited to continue the displacement time series of more than 60~70% of ERS-SAR PS, despite of the frequency gap between the two radars. It has been shown that a single PS dataset can be formed using ERS and ENVISAT images with a common ERS master image. Moreover, the joint analysis of ERS and ENVISAT surveys adds new insight on the physical nature of the Permanent

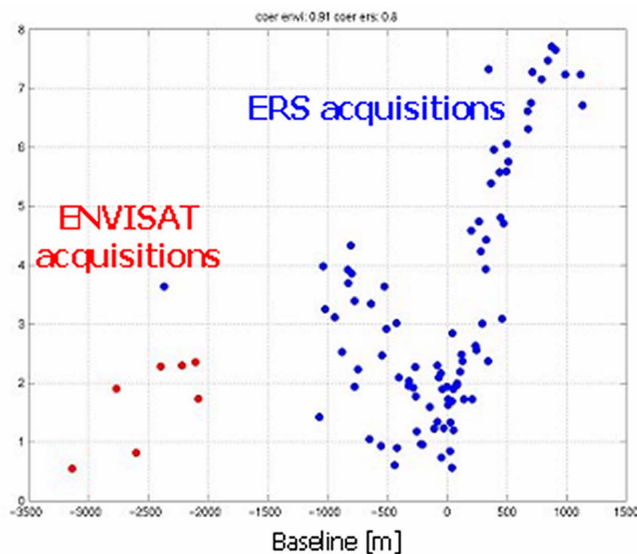


Figure 4. Amplitudes vs baseline, ERS and ENVISAT data relative to a PS.

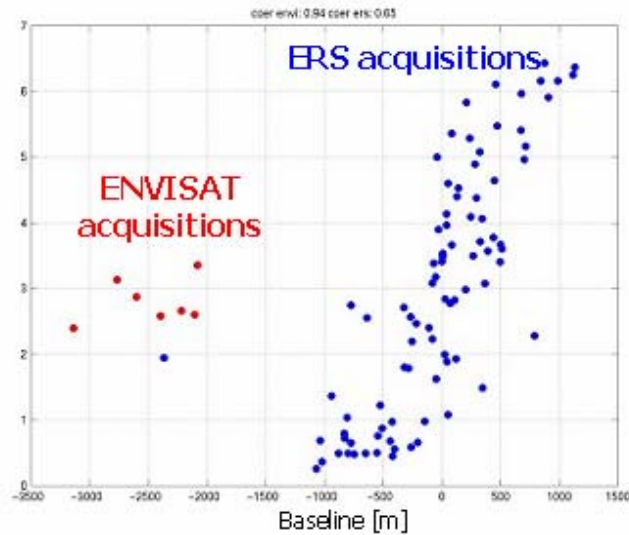


Figure 5. Amplitudes vs baseline, ERS and ENVISAT data relative to a PS.

Scatterers.

ACKNOWLEDGMENTS

The authors are very thankful to ESA for the ENVISAT and ERS data (provided under ESRIN contract No. 16564/02/I-LG) as well as to the whole T.R.E. staff for processing ERS and ENVISAT images.

REFERENCES

[1] A. Ferretti, C. Prati, F. Rocca, "Permanent Scatterers in SAR Interferometry", IEEE TGARS, Vol. 39, no. 1, 2001.

[2] A. Ferretti, C. Prati, F. Rocca, "Non-linear subsidence rate estimation using permanent scatterers in Differential SAR Interferometry", IEEE TGARS, Vol. 38, no. 5, 2000.

[3] C. Colesanti, A. Ferretti, C. Prati, F. Rocca, "Monitoring Landslides and Tectonic Motion with the Permanent Scatterers Technique", Eng. Geology, Vol. 68/1-2, 2003.

[4] Colesanti, C.; Ferretti, A.; Prati, C.; Perissin, D.; Rocca, F., "ERS-ENVISAT permanent scatterers interferometry", Geoscience and Remote Sensing Symposium, 2003. IGARSS '03. Proceedings. 2003 IEEE International, Volume: 2, 21-25 July 2003 Pages:1130 - 1132 vol.2.

[5] M. Arrigoni, C. Colesanti, A. Ferretti, D. Perissin, C. Prati, F. Rocca, "Identification of the location phase screen of ERS-ENVISAT Permanent Scatterers" Proceedings of FRINGE 2003, Frascati (Italy), 1-5 December 2003, ESA SP-550, January 2004.

[6] F. Gatelli et al., "The Wavenumber Shift in SAR Interferometry", IEEE TGARS, Vol. 32, no. 4, 1994.

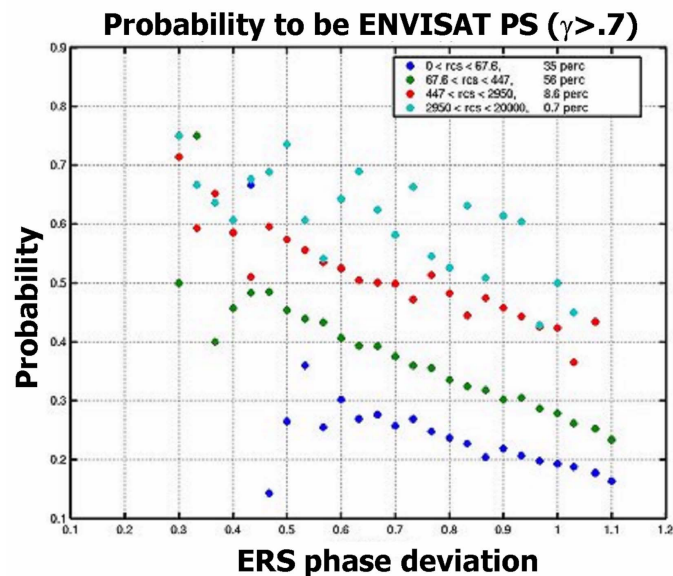


Figure 6. Probability to be a PS in ENVISAT as a function of ERS phase deviation for different RCS classes.